AFRL-VS-TR-2003-1590

VALIDATION OF IONOSPHERIC MODELS

Patricia Doherty

Boston College
Institute for Scientific Research
140 Commonwealth Avenue
Chestnut Hill, MA 02467-3862

31 March 1999

Scientific Report No. 3

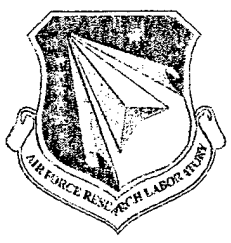

AIR FORCE RESEARCH LABORATORY
Space Vehicles Directorate
29 Randolph Rd
AIR FORCE MATERIEL COMMAND
Hanscom AFB, MA 01731-3010

"This technical report has been reviewed and is approved for publication"

/signed/

JOHN RETTERER
Contract Manager

/signed/

ROBERT MORRIS
Branch Chief

This report has been reviewed by the ESC Public Affairs Office (PA) and is releasable to the National Technical Information Service (NTIS).

Qualified requestors may obtain additional copies from the Defense Technical Information Center (DTIC). All others should apply to the National Technical Information Service (NTIS).

If your address has changed, if you wish to be removed from the mailing list, or if the addressee is no longer employed by your organization, please notify AFRL/VSIM, 29 Randolph Road, Hanscom AFB MA 01731-3010. This will assist us in maintaining a current mailing list.

Do not return copies of this report unless contractual obligations or notices on a specific document require that it be returned.

REPORT DOCUMENTATION PAGE

Form Approved
OMB No. 0704-0188

1. REPORT DATE *(DD-MM-YYYY)*	2. REPORT TYPE	3. DATES COVERED *(From - To)*
31-03-1999	Scientific Report No. 3	April 1998 - March 1999

4. TITLE AND SUBTITLE

VALIDATION OF IONOSPHERIC MODELS

5a. CONTRACT NUMBER
F19628-96-C-0039

5b. GRANT NUMBER

5c. PROGRAM ELEMENT NUMBER
61102F

6. AUTHOR(S)

Patricia H. Doherty

5d. PROJECT NUMBER
1010

5e. TASK NUMBER
IM

5f. WORK UNIT NUMBER
AC

7. PERFORMING ORGANIZATION NAME(S) AND ADDRESS(ES)

Boston College / Institute for Scientific Research
140 Commonwealth Avenue
Chestnut Hill, MA 02467-3862

8. PERFORMING ORGANIZATION REPORT NUMBER

9. SPONSORING/MONITORING AGENCY NAME(S) AND ADDRESS(ES)

Air Force Research Laboratory/VSBXP
29 Randolph Road
Hanscom AFB, MA 01731-3010

10. SPONSOR/MONITOR'S ACRONYM(S)

11. SPONSOR/MONITOR'S REPORT NUMBER(S)
AFRL-VS-TR-2003-1590

12. DISTRIBUTION/AVAILABILITY STATEMENT

13. SUPPLEMENTARY NOTES

Approved for public release; distribution unlimited.

14. ABSTRACT

During the period of April 1998 through March 1999, research efforts continued to support the validation of ionospheric models. These efforts included the acquisition and analysis of ionospheric measurements, software and algorithm development and comprehensive analysis of ionospheric model results. Research results provided unique TEC, scintillation and electron density data sets for model validations. Efforts also provided initial validations of a new sensor's ability to measure the electron density profile, novel applications of kinetic equations for ionospheric modeling, and the first comprehensive validation and comparison of various climatological and assimilative ionospheric models. The work resulted in five presentations at ionospheric conferences and one published journal article.

15. SUBJECT TERMS

Ionosphere, Pseudorange errors, Scintillation, Electron density, Global Positioning System (GPS)

16. SECURITY CLASSIFICATION OF:			17. LIMITATION OF ABSTRACT	18. NUMBER OF PAGES	19a. NAME OF RESPONSIBLE PERSON
a. REPORT	b. ABSTRACT	c. THIS PAGE			John Retterer
U	U	U	SAR	21	19b. TELEPHONE NUMBER *(Include area code)* 781-377-3891

TABLE OF CONTENTS

1. GOALS

The objective of this contract is to obtain various ionospheric measurements from a wide range of geographic locations and to utilize the resulting databases to validate the theoretical ionospheric models that are the basis of the Parameterized Real-time Ionospheric Specification Model (PRISM) and the Ionospheric Forecast Model (IFM).

In this past year, we have supported these goals with the following activities:

- a validation of the ionospheric inversion algorithms of the NPOESS/GPSOS type sensor.
- the preparation and application of GPS/MET data for model validations.
- the application of plasma kinetic equations for ionospheric modeling.
- algorithm development to define single frequency GPS positioning errors.
- characterization of phase scintillation using dual-frequency GPS measurements.
- comprehesive validation and comparison of several ionospheric climatological and weather specification models using various ionospheric databases.

These activities resulted in four presentations at ionospheric conferences and one published journal article. Details of these activities, presentations and publication are provided in this report.

2. PROGRESS

2.1 Validation of Ionospheric Inversion Algorithms with NPOESS/GPSOS Type Sensor

In the previous year, efforts to validate the lower portions of the electron density profiles (EDP) derived from Abel inversions of GPS/MET occultations were initiated. That work included finding coincidences between GPS/MET occultations and ground-based digisondes. In the present year, we have continued to build the database of coincident GPS/MET and digisonde measurements. To date, we have acquired, processed and analyzed 21 cases for both day and night in the American and Brazilian sectors.

In the current year, we have further supported this effort by providing data to validate the topside of the EDPs provided by the NPOESS/GPSOS sensor. The inversion process used in the sensor produces a profile that extends up through the topside up to the altitude of the satellite making the occultation observations. In order to begin validating the ability of the inversion algorithms to produce accurate topside EDPs, we have examined coincidences between GPS/MET occultations and the DMSP, F12 and F13 satellites. By comparing the total ion density measured by the Retarding Potential Analyzer (RPA) onboard the DMSP satellites and that inferred from the GPS/MET derived EDP, we perform the first validations for a variety of ionospheric conditions of the topside portion of GPS/MET based EDPs.

In the current year, we examined 51 cases, 22 at mid-latitudes and 29 at low-latitudes. On average, the GPS/MET inferred densities are within 15 percent of the DMSP observations. Given that the comparisons between incoherent scatter radar (ISR) and DMSP have had around 20 percent agreement and that comparisons between the two instruments on DMSP that measure total ion density agree to around 10 percent, we conclude that this 15 percent agreement is an excellent result. One measure of the spread about the mean behavior is given by the fact that fewer than 80 percent of the 51 cases are within 20 percent of the DMSP observations. For contrast, if we used climatology as given by PIM to predict the DMSP measurements, we find that only 14 percent of the cases would fall within 20 percent of the DMSP observations.

In the current year, efforts were also made to enhance and develop software to process the GPS/MET occultation data. Enhancements included the ability to handle occultations for both rising and setting GPS satellites and to automate much of the data analysis process. In addition, software was developed to search the database for specific criteria and to graphically display the results.

The results of this year's efforts were presented at the Jet Propulsion Laboratory Altimetry Workshop:

> D.N. Anderson, D.T. Decker, F.J. Rich, P.H. Doherty and C. Rocken, 1998, "GPS/MET Occultations: Validation of Ionospheric Inversion Techniques Through Comparisons with Ground-Based and Satellite Sensor Observations," presented at the Jet Propulsion Laboratory (JPL) Altimetry Workshop, Pasadena CA.

2.2 Ionospheric Modeling Using Systems of Plasma Kinetic Equations

Software has been developed to find the solution to the ion kinetic equation for ions moving in both the positive and negative directions. The software used the split operator method to divide the differential equation into three parts. Two of the parts were solved using analytic methods. An unsuccessful attempt was made to find an analytic method for the third part. Further analysis will continue in an effort to solve for the third part of the equation.

2.3 Determination of Position Errors for Single-Frequency GPS Receivers

Mathematical analysis was performed to investigate navigational position errors caused by inaccuracies in the standard Ionospheric Correction Algorithm (ICA) used by all single-frequency GPS receivers. The ICA, developed in the 1970's was designed to correct for 50 percent of the delay on pseudoranges introduced by the ionosphere. Therefore, in many cases, a residual delay error remains on each pseudorange. Errors like these, were computed by comparing the ICA estimate with measured and modeled ionospheric values. These errors were then propagated through the solution process to determine the navigation position error. The most significant impact occurs when a

gradient exists in the pseudorange errors, with the least importance on their magnitude. Horizontal errors of 10, 25 and 40 meters are possible in equatorial latitudes for solar minimum, moderate and maximum conditions, respectively. The largest errors are generally confined to equatorial regions where sharp ionospheric gradients, caused by the equatorial anomaly, frequently occur. Comparing these results with differences in positional data recorded by co-located single and dual-frequency GPS receivers on Ascension Island has produced preliminary and successful validation of this method.

This work was completed in the current year and is currently being prepared for presentation at the Ionospheric Effects Symposium to be held in May 1999 and at the Institute of Navigation conference to be held in June 1999.

2.4 Characterization of Phase Scintillation using Dual-Frequency GPS Measurements

The scintillation of radio signals due to their propagation through ionospheric irregularities is fast becoming a very important issue for GPS receivers operating in equatorial regions where these irregularities are most frequently severe. Irregularities in the electron content of the equatorial ionosphere have scale lengths ranging from a few meters to many kilometers, and can cause diffraction and refraction of the GPS signals. These effects give rise to temporal fluctuations in the signal amplitude and phase at the receiver and are referred to as scintillation.

In the current year, efforts were made to quantify and understand the effects of scintillation at GPS frequencies at an equatorial location. These efforts included the acquisition and processing of GPS measurements recorded at Ascension Island (7.95° south and 14.41° west) from 1 February 1998 through 7 April 1998. The process included characterizing the phase scintillation experienced by this GPS data set by measuring the time Rate Of TEC (ROT) Change in the differential phase of the GPS signals. Further processing included correlating the ROT values with independent measurements of amplitude scintillation.

The results of the Ascension Island study are being prepared for presentation and publication in the next year of this contract.

Similar analysis was applied to a GPS data set recorded in Ny Alesund, Svalbard over the period 4-15 January 1997. This analysis was included in a study to determine the characteristics of plasma structuring in the cusp/cleft region at Svalbard during a magnetically active period. The results of this work are summarized in the following paper (see Appendix):

> Basu, S. Weber, E.J., Bullett, T.W., Keskinen, M.J., MacKenzie, E., Doherty, P., Sheehan, R., Kuenzler, H., Ning, P. and Bongiolatti, J., 1998, "Characteristics of Plasma Structuring in the Cusp/Cleft Region at Svalbard," *Radio Science*, ***Vol. 33***, Number 6, pp. 1885-1899.

2.5. Validation and Comparison of Ionospheric Models

A comprehensive effort to validate and compare several climatological ionospheric models was initiated in the current year. This study was initiated to establish the baseline capability of an array of ionospheric models currently in use. The initial efforts of this study focused on climatological models, such as PIM, IRI, BENT and RIBG. Later work focused on weather specification models, such as PRISM, GTIM, IFM and CITEFM.

These efforts utilized a variety of datasets, both ground-based and satellite-based, to assess how well the various models represent the climatology and weather contained in the datasets. In the current year, we assembled a database of TEC measurements recorded in Taiwan and Massachusetts over a full solar cycle. These measurements were representative of long-term ionospheric behavior in low- and mid-latitude locations. In addition, we prepared TEC measurements recorded at Ascension Island between 1980 and 1981. These measurements being characteristic of near worst case ionospheric behavior that occurs in the near-equatorial region during peak solar activity. Finally, we prepared foF2 and hmF2 measurements recorded at Boulder CO over a five year period from 1986-1990.

Figure 1 shows the results obtained in the current year for the validations of PIM and IRI TEC using the Ascension Island data. In this figure, we have plotted the monthly mean TEC recorded at Ascension Island for each of the 16 months between January 1980 and April 1981. Note that the measured data is plotted in black. The modeled TEC from PIM and IRI are overplotted in red and blue respectively. The results illustrate that both models tend to overestimate the nighttime data, particularly during the equinoctial months of March, April, September and October. The figure also shows that the PIM model performs better during the equinoctial daytime hours. Both models underestimate winter daytime and do a fairly accurate estimation during summer daytime.

Figure 2 shows the results obtained for the validations of foF2 in PIM and IRI using the Boulder data. Note that the results are plotted as the monthly mean value for January, March, June and September for the years of 1986 through 1990. Note that the IRI model shows better performance for foF2 estimations than does the PIM model.

The techniques used in our validation efforts together with the initial results were presented as follows:

> Doherty, P., Sultan, P.J., Decker, D.T., Borer, W.S., Daniell, R.E., and Brown, L.D., 1998, "Validation of Ionospheric Models," presented at AGU Fall Meeting, San Francisco CA.

Further analysis was performed and was prepared for presentation in the next year of this contract. These developments included the validation and comparison of the RIBG and BENT models.

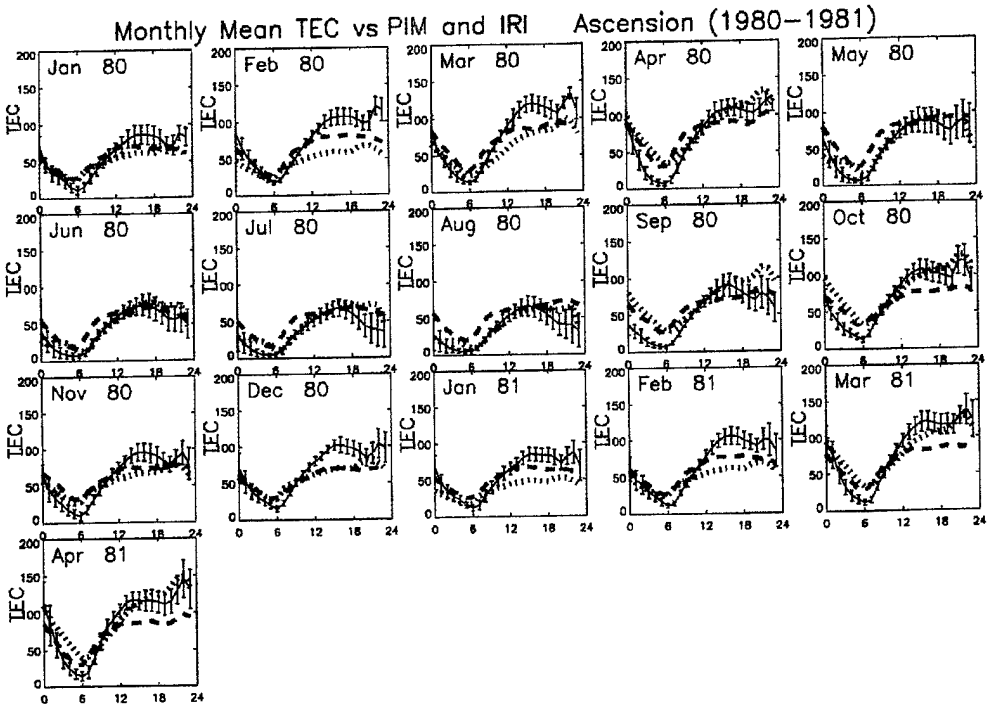

Figure 1. Monthly Mean TEC Recorded at Ascension Island versus PIM and IRI Modeled TEC.

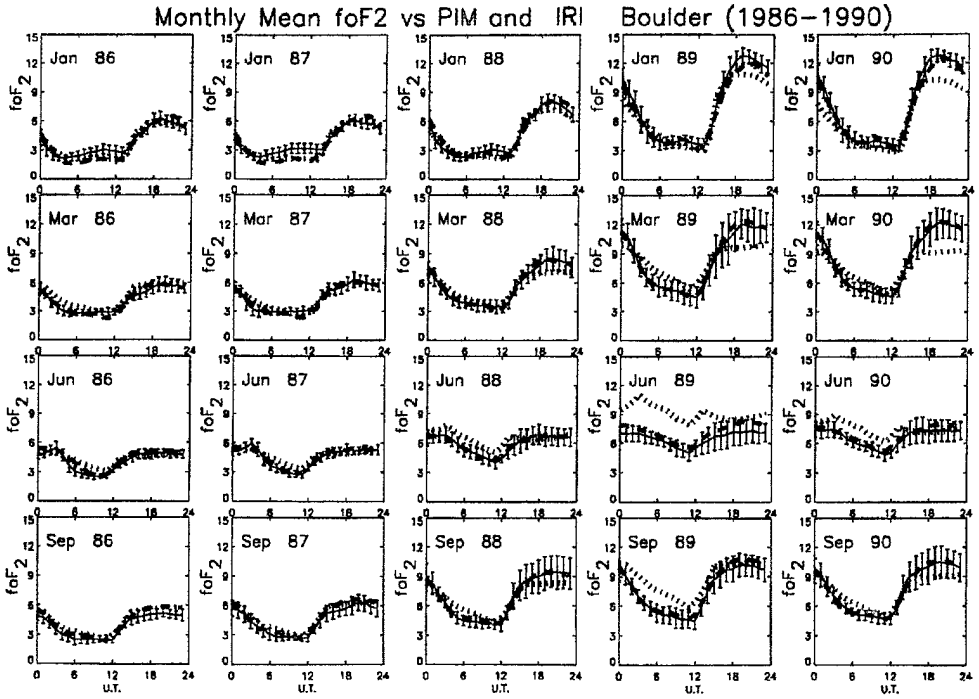

Figure 2. Monthly Mean foF2 Recorded at Boulder versus PIM and IRI Modeled foF2.

3. PRESENTATIONS

Doherty, P.H., Sultan, P.J., Decker, D.T., Borer, W.S., Daniell, R.E., and Brown, L.D., 1998, "Validation of Ionospheric Models," presented at AGU Fall Meeting, San Francisco CA.

Anderson, D.N., Decker, D.T., Rich, F.J., Doherty, P.H. and Rocken, C., 1998, "GPS/MET Occultations: Validation of Ionospheric Inversion Techniques Through Comparisons with Ground-Based and Satellite Sensor Observations," presented at the Jet Propulsion Laboratory (JPL) Altimetry Workshop, Pasadena CA.

Decker, D.T., Doherty, P.H., Anderson, D.N., Rich, F.J., and Rocken, C., 1998, "GPS Occultation: A New Remote Sensing Technique for the Ionospheric Topside?," presented at the 1998 Spring AGU Meeting, Boston MA

Groves, K.M., Basu, S., Quinn, J., Kuenzler, H., Bishop, G., Doherty, P., and Ning, P., 1999, "A Comparison of TEC Fluctuations and Scintillations at Ascension Island," presented at the National Radio Science Meeting, Boulder CO.

4. JOURNAL ARTICLES

Basu, S., Weber, E.J., Bullett, T.W., Keskinen,M.J., MacKenzie, E., Doherty, P., Sheehan, R., Kuenzler, H., Ning, P., and Bongiolatti, J., 1998, "Characteristics of Plasma Structuring in the Cusp/Cleft Region at Svalbard," *Radio Science*, ***Vol. 33***, Number 6, pp. 1885-1899.

APPENDIX

Radio Science, Volume 33, Number 6, Pages 1885–1899, November–December, 1998

Characteristics of plasma structuring in the cusp/cleft region at Svalbard

S. Basu,[1] E. J. Weber,[1] T. W. Bullett,[1] M. J. Keskinen,[2] E. MacKenzie,[3] P. Doherty,[3] R. Sheehan,[3] H. Kuenzler,[1] P. Ning,[4] and J. Bongiolatti[1]

Abstract. Satellite scintillation, all-sky optical imager, and digisonde observations were coordinated during a cusp campaign conducted at Ny Alesund, Svalbard (78.9°N, 11.8°E; 75.7°N corrected geomagnetic latitude, over the period January 4–15, 1997. This paper is focused on a study of the distribution and dynamics of mesoscale (tens of kilometers to tens of meters) electron density irregularities in the dayside auroral region. This study has been performed at Ny Alesund, Svalbard, by measuring the effects of these irregularities on the amplitude scintillation of 250-MHz transmissions from a quasi-stationary polar satellite as well as the amplitude and phase scintillation of 1.6-GHz signals from Global Positioning System (GPS) satellites. These GPS scintillation measurements were augmented by the use of dual-frequency (1.2 and 1.6 GHz) GPS phase data acquired at the same station by the Jet Propulsion Laboratory for the International GPS Geodynamic Service (IGS). The continuous 250-MHz scintillation observations explored the daytime auroral ionosphere 2° poleward of Ny Alesund and showed that the scintillation spectra are often broad, as may be expected for irregularities in a turbulent flow region. Such irregularity dynamics were detected poleward of the nominal cusp region over the interval of 0600–1500 magnetic local time. The period of observations included the magnetic storm of January 10–11, 1997, when GPS observations of the IGS detected polar cap patches with total electron contents of 3×10^{16} m^{-2} and large-scale (tens of kilometers) phase variations at the GPS frequency of 1.6 GHz that corresponded to temporal gradients of 2×10^{16} m^{-2} min^{-1}. However, amplitude scintillations at the GPS frequency of 1.6 GHz could not be detected in association with these large-scale phase variations, indicating that the irregularities with wavelengths less than the Fresnel dimension of 400 m were below the detectable limit. This is shown to be consistent in the context of enhanced ionospheric convection determined by digisonde and scintillation spectra.

1. Introduction

The cusp/cleft region [*Newell and Meng*, 1992] in the dayside auroral oval is recognized to be the seat of structured electric fields, soft particle precipitation, large plasma flows, and auroral break-up events [*Sandholt et al.*, 1990; *Smith and Lockwood*, 1990]. These dayside auroral signatures are probed by multitechnique observations to investigate the coupling processes within the solar wind–magnetosphere–ionosphere system. From the standpoint of plasma structuring, the dayside auroral oval may be considered as the source region and gateway of major irregularity structures in the high-latitude ionosphere.

It is well established that the dayside auroral oval plays a major role in the formation of large-scale ionization structures, called patches, in the polar ionosphere [*Buchau et al.*, 1983; *Weber et al.*, 1984]. A great deal of research has revealed that under active magnetic conditions, the eastward electric field in the dayside auroral oval directs a "tongue of ionization" from the subauroral region into the polar cap which is sliced off into discrete structures by high plasma flows [*Tsunoda*, 1988; *Valladares et al.*, 1994, and references therein]. The convecting patches develop intermediate scale (tens of kilometers to tens of meters) irregularities by the action of the gradient drift instability mechanism [*Chaturvedi and Huba*, 1987; *Tsunoda*, 1988, and references therein]. This was confirmed experimentally by showing that patches are

[1] Air Force Research Laboratory, Hanscom Air Force Base, Massachusetts.
[2] Plasma Physics Division, Naval Research Laboratory, Washington, D. C.
[3] Institute for Scientific Research, Boston College, Newton, Massachusetts.
[4] KEO Consultants, Brookline, Massachusetts.

Paper number 98RS01597.
0048-6604/98/98RS-01597$11.00

associated with scintillations of satellite signals which arise from the scattering of radio waves from intermediate scale irregularities [*Weber et al.*, 1986]. Indeed, after weak scintillation events due to polar cap arcs are excluded, the statistics of the remaining strong scintillation events in the polar cap [*Aarons et al.*, 1981; *Basu et al.*, 1985; *Kersley et al.*, 1995] may be used as the statistics of polar cap patches.

In addition to patches which convect into the polar cap, the sheared electric field in the cusp/cleft region is a viable source of localized intermediate scale (tens of meters to tens of kilometers) irregularities. *Basu et al.* [1988] first identified irregularities in velocity shear regions associated with nightside auroral arcs and provided a comprehensive description of the density and electric field fluctuation spectra. This stimulated theoretical development of instabilities driven by velocity shears parallel and perpendicular to the magnetic field [*Keskinen et al.*, 1988; *Basu and Coppi*, 1990; *Ganguli et al.*, 1989]. Compared with convective instabilities at high latitudes, the irregularities generated in velocity shear regions exhibit strikingly enhanced electric field fluctuations for given relative density fluctuations. Scintillations of satellite signals due to irregularities in the velocity shear region are expected to be weaker than patch-induced scintillations since patches are associated with high plasma density. However, the enhanced electric field fluctuations are expected to broaden the frequency spectra of scintillations as well as the Doppler spectra of HF backscatter.

In this paper we present the results of 250-MHz scintillation observations made from Ny Alesund, Svalbard (78.9°N, 11.9°E; corrected geomagnetic latitude (CGMLAT) 75.7°N, 113.8°E), during the period January 5–15, 1997. The station latitude corresponds to the nominal cusp location, and the station crosses local magnetic noon at 0850 UT. We focus our attention on dayside auroral observations made during 0500–1300 UT. During these hours the propagation path to the satellite explored the ionospheric *F* region about 2° poleward of the station. Spectral studies of 250-MHz scintillation are performed to determine the dynamics of 1-km to 100-m scale irregularities. These scintillation observations are supported by all-sky imager and digisonde observations, as well as scintillation and total electron measurements by the use of Global Positioning System (GPS) satellites. This paper also discusses the plasma structures at various scales encountered during the major magnetic storm of January 10–11, 1997.

2. Experimental Observations

Scintillation measurements were performed at Ny Alesund by the use of 250-MHz transmissions from quasi-stationary beacon satellites. The receivers sample signal intensity at 50 Hz and process the signals on-line to determine the scintillation index (S_4), defined as the normalized second moment of the signal intensity, the frequency spectra, and the distribution function. These parameters are obtained every 82 s and are then averaged to provide values at 5-min intervals. A GPS receiver at L1 (1.575 GHz), manufactured by Novatel, was deployed which acquires amplitude and phase at 50 Hz and obtains phase and amplitude scintillation at 82-s intervals. Dual-frequency GPS data were obtained from the Ny Alesund station of the International GPS Geodynamic Service (IGS), managed by the Jet Propulsion Laboratory. The IGS data provide 30-s values of carrier phase and group delay at both the GPS L1 (1.6 GHz) and L2 (1.2 GHz) frequencies. The data are processed to obtain the total electron content and the rate of change of the total electron content at 30-s intervals [*Doherty et al.*, 1994]. The all-sky imager mapped the dayside aurora at 630.0 nm and defined the optical auroral conditions at the subionospheric location which was probed by continuous 250-MHz scintillation measurements. The study is focused on daytime observations between 0800 and 1500 MLT, when the subionospheric location remained at about 78° CGMLAT, 2.3° poleward of Ny Alesund. Since Ny Alesund corresponds nominally to the dayside cusp region, this poleward position of scintillation observations during the daytime may be identified with the mantle region [*Newell et al.*, 1991].

3. Results and Discussions

Figure 1 shows the geometry of 250-MHz scintillation observations from Ny Alesund. The location of the station (75.7° CGMLAT) at magnetic noon (0850 UT) is indicated by a cross. The loci of the 350-km subionospheric position of scintillation observations with quasi-stationary satellites at different universal times (UT) are indicated at hourly intervals by asterisks and diamonds, which correspond to the two satellites. During this period the station will, of course, trace out a circular path, which is not shown in order to ensure clarity of the diagram; instead, its position at one particular time (0845 UT) corresponding to magnetic noon has been illustrated. Observations with each satellite are made for about 6

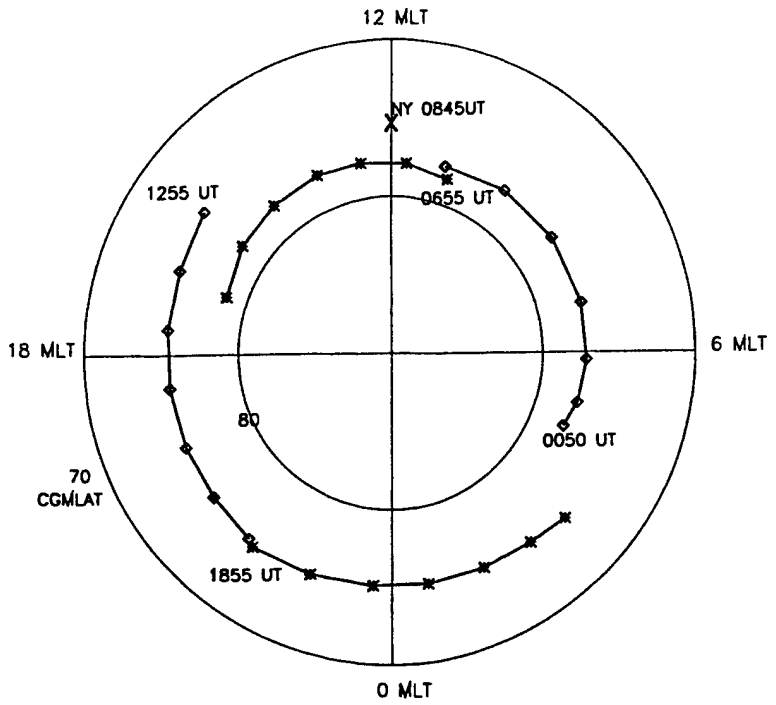

Figure 1. Shown is the geometry of 250-MHz scintillation observations in magnetic local time and the corrected geomagnetic latitude (CGMLAT) coordinate system. The measurements were made from Ny Alesund, Svalbard (CGMLAT 75.7°N) by using quasi-stationary beacon satellites. The position of the station is only shown at magnetic noon and is indicated by a cross. The 350-km subionospheric intersections of scintillation measurements at hourly universal time intervals are shown by crosses and diamonds.

hours, after which they are switched to the next available satellite. Although scintillation observations were performed around the clock, we shall focus in this paper on the results obtained during about 4 hours on either side of magnetic noon. Figure 1 shows that during this period, namely, 0500–1300 UT, scintillation observations probed the ionosphere at 78° CGMLAT, which, as mentioned above, is approximately 2° poleward of Ny Alesund.

We shall now discuss the characteristics of 250-MHz scintillation in the dayside auroral region with the typical example of January 6, 1997. It was a magnetically quiet day, as were most of the days during the campaign period. The Wind satellite data indicated that over the study period of 0500–1300 UT, the interplanetary magnetic field (IMF) B_z was southward, with $B_z = -2$ nT for only 1 hour between 0900 and 1000 UT, and remained northward for the rest of the period with values ranging between +2 and +3 nT. Figure 2 shows the 630.0-nm images obtained by the all-sky imager at Ny Alesund at 1-min intervals between 0954 and 0958 UT. The 180° field-of-view images are presented in all-sky lens coordinates, with a linear change in elevation angle from 90° at the center to 0° at the edge of the image. The top, bottom, right and left of each image represent the four cardinal directions, north, south, east and west, respectively. The images show the stable cusp aurora, which are characterized by a rather sharp equatorward edge and a markedly diffuse poleward edge [*Maynard et al.*, 1997]. The asterisks in these images represent the directions of the propagation path of satellite scintillation observations. These images indicate that the propagation path intersected the cusp plume poleward of the cusp [*Newell et al.*, 1991]. At this time, no optical emission at 427.8 nm was ob-

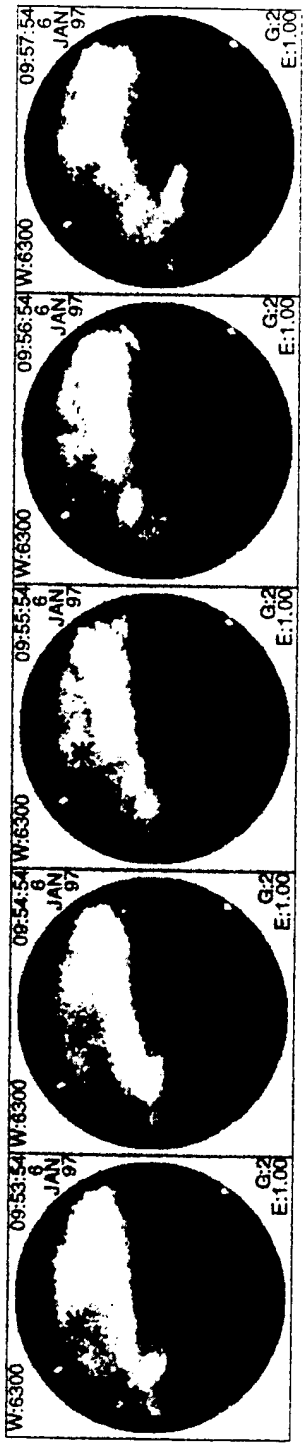

Figure 2. All-sky imager observations of the emissions at 630.0-nm wavelengths at each minute. The four cardinal directions, north, south, east, and west, correspond to the top, bottom, right, and left edges of the images. The observations are from Ny Alesund, Svalbard, on January 6, 1997. The elevation and azimuth of scintillation observations are indicated by asterisks in the images.

served, indicating that only soft particle precipitation was associated with the 630.0-nm images.

Figure 3 illustrates the variation of the S_4 index of amplitude scintillation with UT as recorded on January 6, 1997. The S_4 index, obtained from the ratio of the standard deviation of signal intensity fluctuation normalized to the average signal intensity, quantifies the strength of amplitude scintillation. In view of the prevailing solar minimum condition, scintillations were weak and did not exceed the weak scatter limit of $S_4 = 0.5$. Figure 3 clearly illustrates the daytime scintillation activity between 0500 and 1300 UT, with minimum S_4 values increasing to 0.2 and individual events increasing to 0.4. It establishes the presence of subkilometer scale irregularities during daytime at 78° CGMLAT over an extended magnetic local time interval of 0845–1645 MLT. Considering the optical images shown in Figure 2, the narrow scintillation structure around 1000 UT in Figure 3 is to be associated with the cusp plume. Scintillations, however, are continuously observed over most of the daytime at locations poleward of the dayside auroral oval corresponding to the mantle region. *Kersley et al.* [1995] obtained the occurrence statistics of phase scintillation from Ny Alesund and showed that large-scale (>10 km) irregularities occur during much of the daytime and are distributed in a belt extending from the south to the north of the station.

We now illustrate that the frequency spectra of daytime amplitude scintillations observed slightly poleward of the cusp have very special characteristics. Figure 4 shows a set of four successive spectra at 5-min intervals. Each of these spectra is obtained by using the fast Fourier transform (FFT) algorithm averaged over four successive 82-s data segments. These samples were obtained near magnetic noon, and the spectra show the variation of the power spectral density (psd) in decibels with log frequency. Each spectrum is characterized by a flat low-frequency portion and then a linear roll-off at higher frequencies, indicating a power law variation of psd with frequency. It is to be noted that the scintillation index of all the samples conforms to weak scatter limit ($S_4 < 0.5$). Under these conditions the power spectrum is expected to show a maximum at the Fresnel frequency (f_F), above which the spectrum should roll off rapidly and below which the spectrum should again roll off but at a much shallower slope [*Basu et al.*, 1994]. The Fresnel frequency is given by $f_F = v/(2\lambda z)^{1/2}$, where v is the irregularity drift perpendicular to the propagation path, λ is the radio

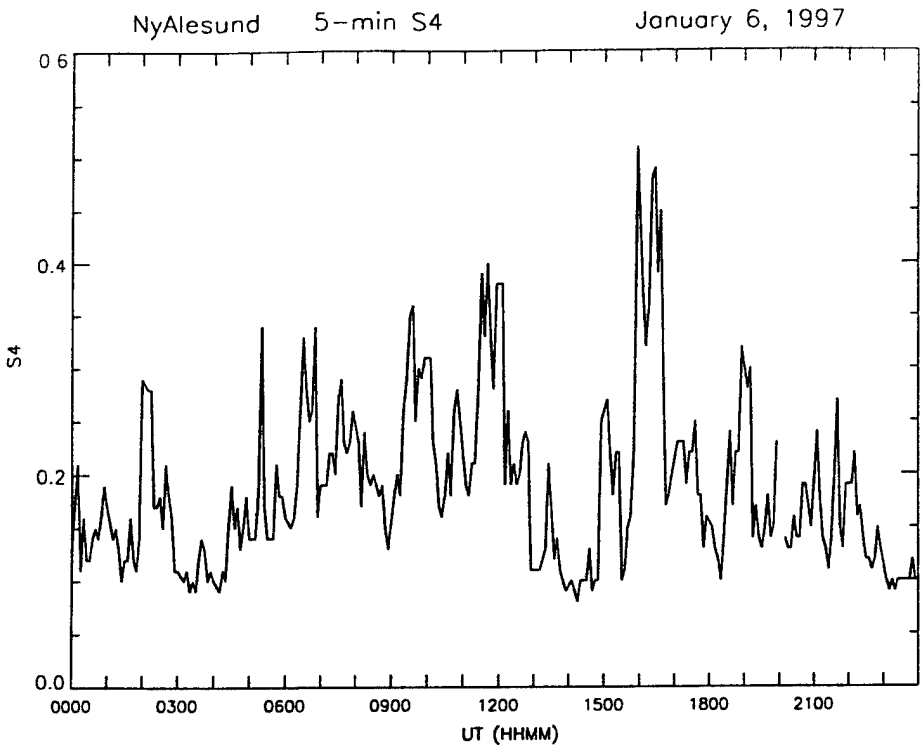

Figure 3. Shown is the observed variation of the S_4 index of scintillation at 250 MHz with universal time as observed on January 6, 1997. The S_4 index of scintillation is defined as the normalized second moment of signal intensity. The measurements were performed from Ny Alesund, Svalbard. The observing period of 0400–1400 UT corresponds to dayside auroral measurements.

wavelength, and z is the slant range to the irregularity layer. The spectral set in Figure 4 does not conform to the weak scatter spectral specifications for uniform flow speed. Instead, the flat-topped low-frequency spectral form may be a result of the irregularities moving with a distributed velocity rather than a uniform flow speed [*Lotova*, 1981]. The corner frequencies of the spectra shown in Figure 4 vary from one spectra to another, indicating that the velocity dispersion is a function of space and time. Figure 5 illustrates two spectra from the early morning period that indicate the shape of a weak scintillation spectrum in a uniform flow region. In this case, the spectra have narrower bandwidths and exhibit spectral maximum, particularly noticeable in the left-hand (0204:54 UT) spectrum, and have steeper high-frequency roll-off, with power law spectral indices of about 3 as compared with power law indices of 2 in Figure 4. Finally, it is to be emphasized that the broadband spectra shown in Figure 4 are observed just poleward of the cusp, not only at magnetic noon but over an extended period during the daytime. However, the signature of velocity dispersion is most enhanced around magnetic noon. In a recent comprehensive study of the cusp, *Baker et al.* [1995] have established that HF radar backscatter from the cusp exhibits wide and complex Doppler spectra. This result implies that the cusp is a region of high electric field turbulence which is in agreement with the DE 1 and DE 2 satellite data [*Maynard et al.*, 1991; *Basinska et al.*, 1992].

Another example of daytime scintillation at 250 MHz is shown in Figure 6. A clear commencement of a scintillation event at 0500 UT and the decay at 1200 UT may be noted. The campaign ended at 1200 UT, which caused the abrupt end of the data. The daytime scintillation event again corresponded to the poleward location of about 78° CGMLAT and covered the time interval of about 0900–1600 MLT. The magnitude of scintillation was weak and remained below the S_4 level of 0.3. The scintillation spectra for this event are illustrated in Figure 7. As discussed earlier, the

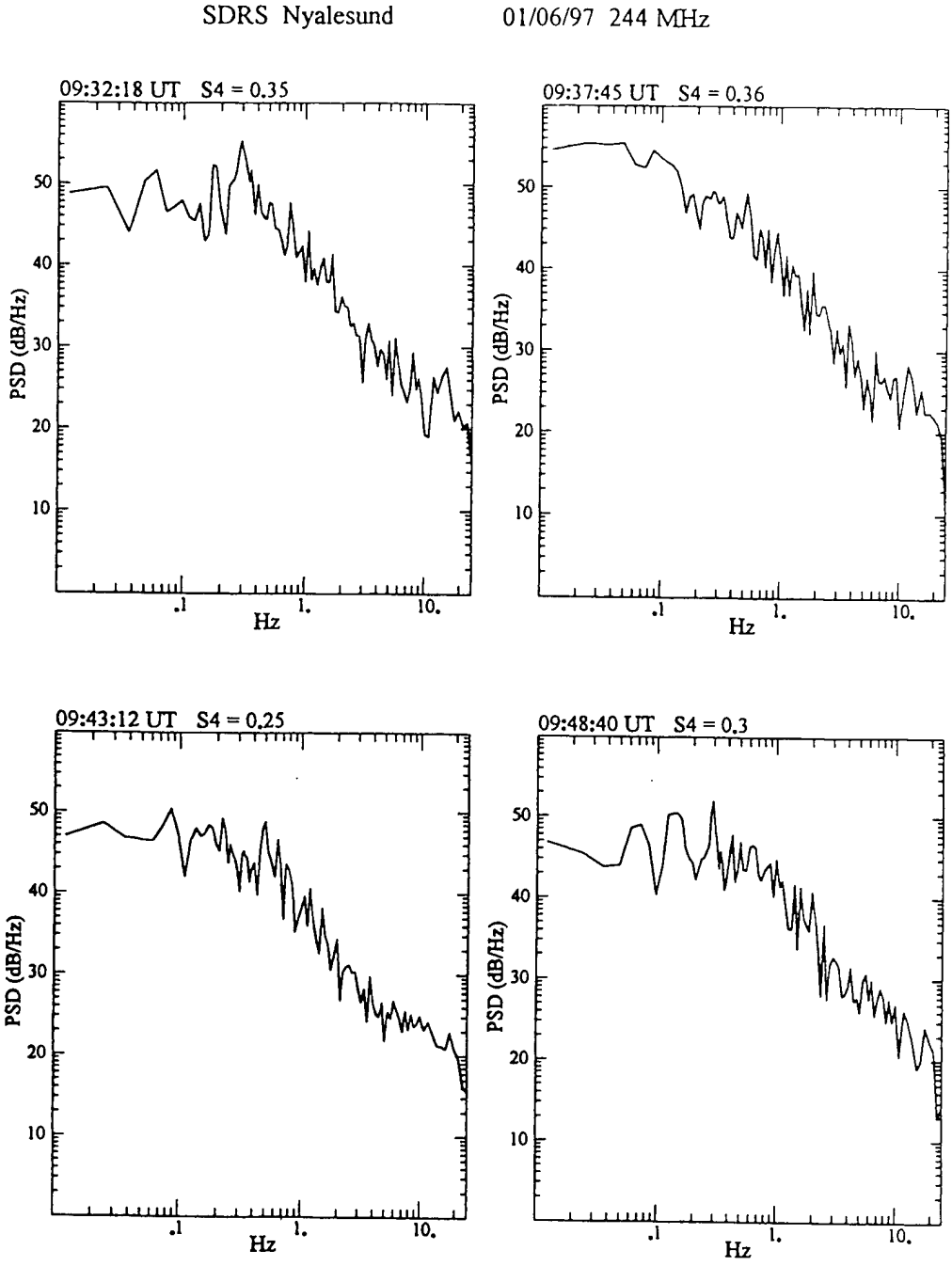

Figure 4. The frequency spectra of 250-MHz scintillations recorded on January 6, 1997, at Ny Alesund, Svalbard, are illustrated at 5-min intervals near magnetic noon. Broad spectra are illustrated.

flat-topped spectra indicate that the irregularities have turbulent velocities. The spectral width is considerably larger compared with the January 6, 1997, spectra, indicating larger velocity dispersion.

During the campaign period a major magnetic storm occurred during January 9–11, 1997. To show the effect of the storm on amplitude scintillations at 250 MHz, the diurnal variations of S_4 with UT during January 10–12, 1997, are shown in Figure 8. The quiet-day pattern of scintillations with enhanced ac-

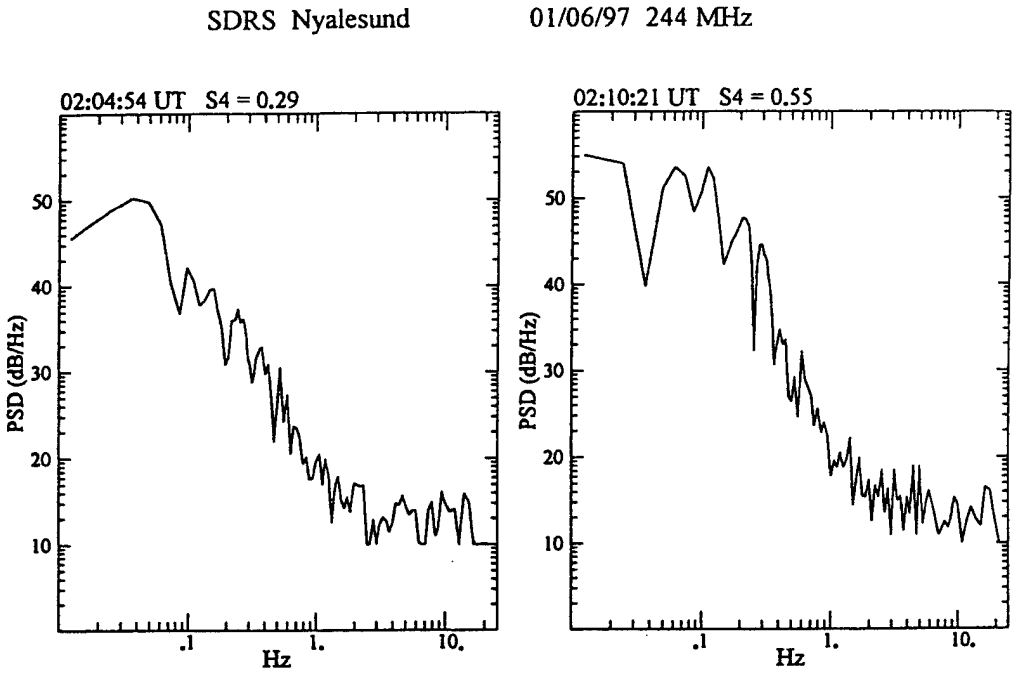

Figure 5. Same as in Figure 4 but obtained during early morning magnetic local time (MLT) hours. Narrowband spectra with Fresnel maximum are illustrated.

tivity around magnetic noon (0850 UT) was observed on January 10 and 12. The pattern changed drastically on January 11, however, when a long enduring prenoon scintillation event during 0000–1000 UT (0400–1400 MLT) was observed, as well as two additional events in the afternoon and early evening period during 1600–2200 MLT. During the prenoon period the Fresnel frequency of scintillation spectra were observed to be as high as 1 Hz. Using the expression given earlier that relates the irregularity drift velocity to the Fresnel frequency, we find that at this time, irregularity drift perpendicular to the propagation path was about 1 km/s. The digisonde at Ny Alesund detected polar cap patches and determined horizontal drifts that increased from 1 km/s at 0000 UT to 1.5 km/s around 0600 UT, which then decreased to about 600 m/s after 1200 UT. These results indicate that the station became a polar cap station due to the expansion of the auroral oval to lower latitudes under these magnetically active conditions, as confirmed by optical images that show no auroral emission within the entire field of view of the imager. This is probably the reason why the diurnal pattern of 250-MHz scintillation on January 11 was distinctly different from other days.

We used the GPS satellite data provided by the IGS station at Ny Alesund to further investigate the patch characteristics. The IGS stations are equipped with dual-frequency (1.2 and 1.6 GHz) GPS receivers and provide differential carrier phase and differential group delay data at 30-s intervals. The GPS data were analyzed to estimate the total electron content (TEC) of the ionosphere and also the magnitudes of large-scale irregularity structures from the rate of change in differential carrier phase, which is equivalent to the rate of change of TEC. The rate of change of TEC is derived from the differential carrier phase data, which are provided at 30-s intervals. The data are filtered to remove variations with periods longer than 15 min, and then the rate of change of TEC is obtained at 1-min intervals from 30-s TEC values. This algorithm was first developed by J. A. Klobuchar and P. Doherty at Phillips Laboratory (now Air Force Research Laboratory) and has now been adapted by various groups for ionospheric studies at low and high latitudes by the use of the widely dispersed IGS network of stations [*Doherty et al.*, 1994]. In a recent paper, *Pi et al.* [1997] have indicated how measurements of the rate of change of TEC by the global IGS network may be exploited to monitor the instantaneous global distribution of ionospheric irregularities. Figure 9 shows the 350-km subionospheric position of

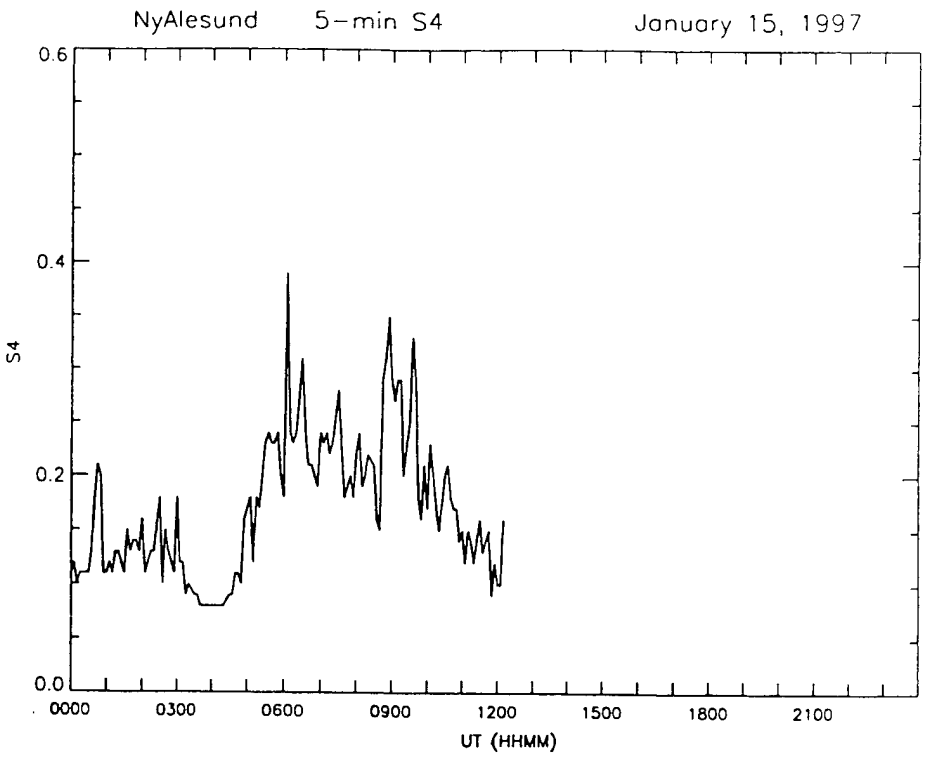

Figure 6. Same as in Figure 3 but performed on January 15, 1997.

GPS satellites, viewed from Ny Alesund, in the day sector between 0600 and 1800 MLT. The diamonds along the tracks signify locations where the rate of change of TEC exceeded 1 TEC unit min^{-1} (1 TEC unit = 10^{16} electrons m^{-2}).

Figure 9 shows that the subionospheric track of satellite prn 26, viewed from Ny Alesund, crossed magnetic noon. The differential carrier phase and group delay data were combined to determine the total electron content. This result is illustrated in Figure 10, which shows the variation of equivalent vertical TEC as a function of universal time. The alternate increases and decreases of TEC signify the transit of polar cap patches across the GPS propagation path. It may be noted that, on average, the patches are associated with an increase of TEC by about 2 TEC units and the patch durations are about 30 min. The patches are very weak because of the prevailing solar minimum condition. The digisonde measurements at Ny Alesund indicated that at this time the horizontal drift is about 600 m s^{-1}. By combining the duration and the drift of the patches, we obtain the horizontal patch dimensions as 1080 km.

The convecting patches develop intermediate scale irregularities through the gradient drift instability mechanism [*Chaturvedi and Huba*, 1987; *Tsunoda*, 1988, and references therein]. With prevailing drift velocities as high as 500–1000 m s^{-1}, patches with relatively gentle spatial gradients of electron density of the order of 50 km, perpendicular to the magnetic field and in the direction of the drift, are expected to become unstable within about a minute and develop intermediate scale irregularities [*Basu et al.*, 1995]. In addition, since the patches may transit through all or part of the cusp enroute to the polar cap [*Sojka et al.*, 1994; *Decker et al.*, 1994], it is conceivable that the patches will be structured in density due to structured cusp electric fields [*Maynard et al.*, 1991; *Basinska et al.*, 1992] or structured particle precipitation from the magnetosheath. The association of density and electric field structures in velocity shear regions at auroral latitudes has been established from satellite in situ measurements [*Basu et al.*, 1988] and accounted for theoretically by several authors [*Keskinen et al.*, 1988; *Basu and Coppi*, 1990; *Ganguli et al.*, 1994]. We discussed earlier the presence of 250-MHz scintillation in the cusp region, which establishes the presence

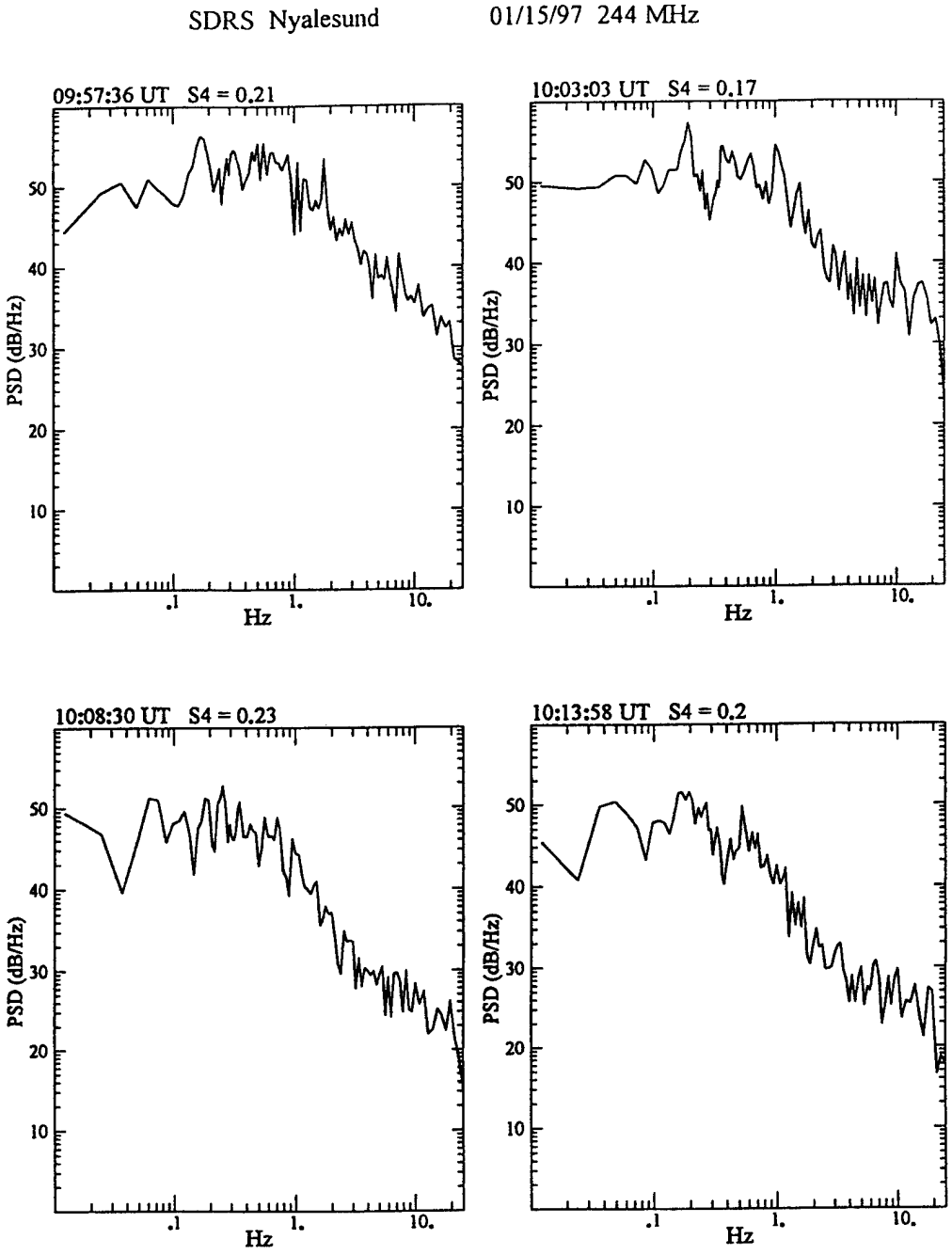

Figure 7. Same as in Figure 4 but on January 15, 1997.

of intermediate scale density irregularities in the range of about 1 km to 100 m. The patches may therefore enter the polar cap after being structured in the cusp at such subkilometer scales. However, since the cusp is localized, these irregularities will decay after the patches exit the source region. The approximate lifetime of the intermediate scale density irregularities in the winter polar cap ionosphere is proportional to the square of irregularity scale size, perpendicular to the geomagnetic field, divided by the electron perpendicular diffusion coefficient. For an altitude of 350 km, 100-m and 1-km scale size density

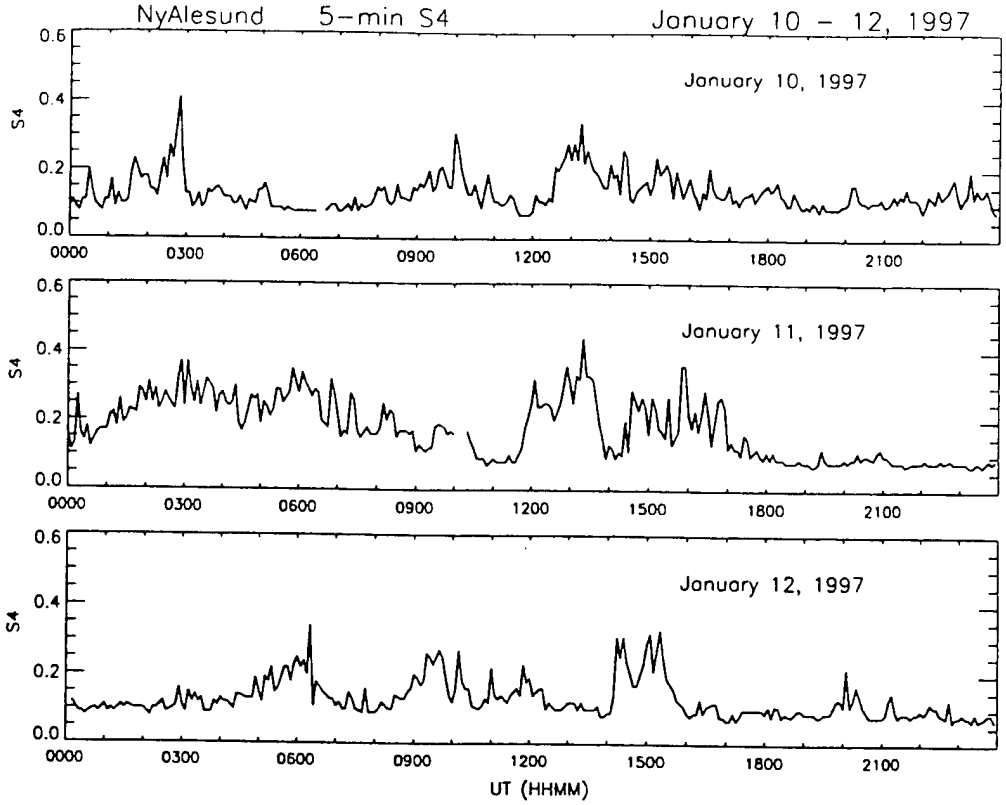

Figure 8. Shown is the variation of S_4 index of scintillation at 250 MHz with universal time observed during the magnetic storm period of January 10–12, 1997. The top and middle panels show the variations during the storm period of January 10 and 11, 1997, respectively, and the bottom panel shows the variation observed on January 12, 1997, immediately after the magnetic storm.

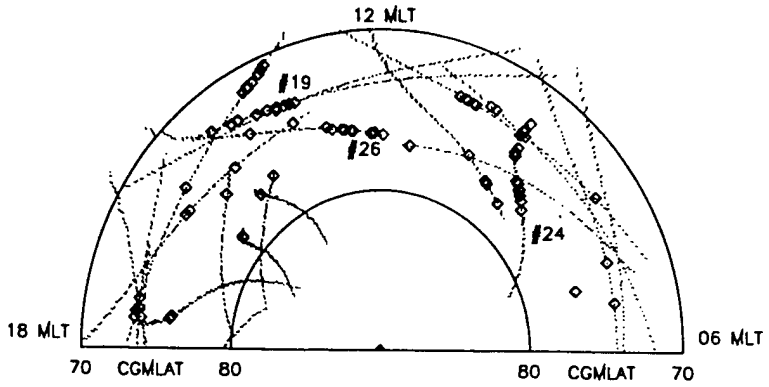

Figure 9. The 350-km subionospheric tracks of Global Positioning System (GPS) satellites as observed from Ny Alesund, Svalbard, on January 11, 1997. The tracks are illustrated in MLT-CGMLAT coordinates. The diamonds indicate that the rate of change of the total electron content (TEC) exceeded 1 TEC unit per minute (1 TEC unit = 10^{16} electrons m^{-2}). Some of these tracks are identified by the corresponding satellite prn's.

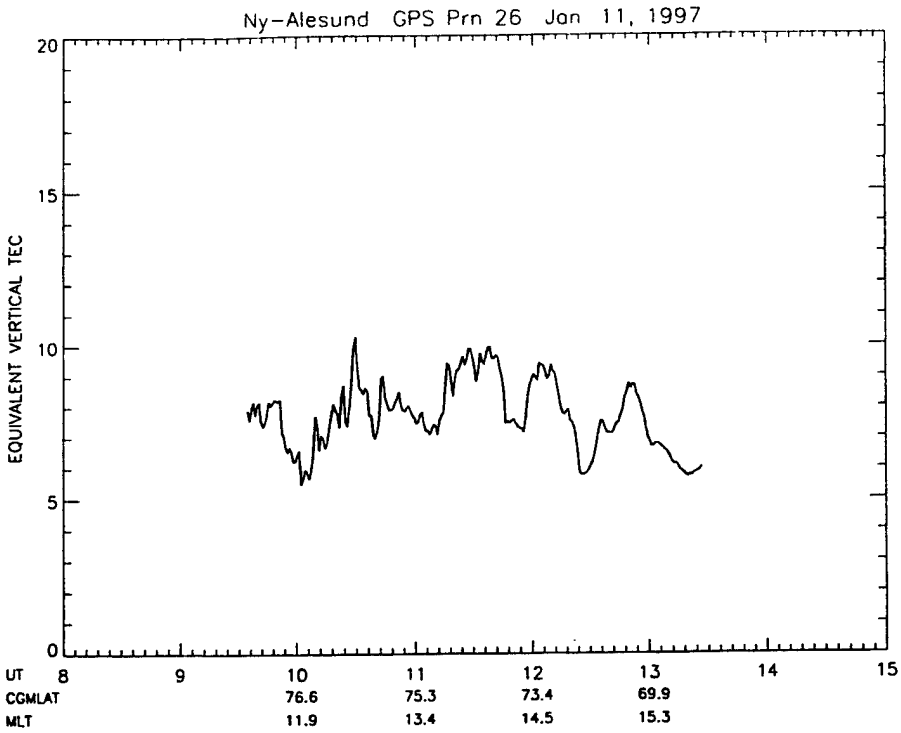

Figure 10. The equivalent vertical total electron content determined during the magnetic storm period of January 11, 1997, using the GPS observations of the International GPS Geodynamic Service (IGS) at Ny Alesund. Patches with about 2 TEC units were detected.

irregularities will decay with typical time constants of the order of minutes and hours, respectively. In view of such long lifetimes of subkilometer scale irregularities, the patches will already be structured when they enter the polar cap. This will contribute to a reduction of the growth time of irregularities in convecting patches by the gradient drift instability mechanism.

We shall now discuss the plasma structuring of patches by determining the rate of change of TEC from two frequencies (1.2 and 1.6 GHz) of GPS satellite observations as well as measuring amplitude scintillations of GPS signals at 1.6 GHz. Figure 11 shows the results of the rate of change of TEC per minute on January 11, 1997, which was determined from the IGS GPS data from Ny Alesund. Each horizontal line represents a GPS satellite with a specific prn and shows phase fluctuations expressed as fluctuations in changes of TEC per minute. The change of 1 TEC unit per minute corresponds to the spacing between the lines in the bottom right corner of the diagram. This representation has been effectively used by *Aarons et al.* [1996] and *Aarons* [1997] for irregularity studies at both equatorial and high latitudes. Figure 11 shows that the satellite (prn 26) recorded changes mostly around ± 1 TEC min^{-1} around 1200 UT when it detected patches. If we recall that the digisonde recorded drifts of 600 m s^{-1} at this time, then the differential carrier phase data with a Nyquist period of 60 s correspond to irregularity wavelengths of 36 km. *Aarons* [1997] has recently performed a careful study of the rate of change of TEC at high latitudes by using the IGS data from 11 high-latitude stations. From this study he concluded that during solar minimum the rate of change of TEC (phase fluctuations) was lower at corrected geomagnetic latitudes >80° as compared with that in the auroral oval. This observation depends on the fact that the phase fluctuations (or the rate of change of TEC) are a function of both change in TEC and the irregularity velocity. It is not clear if the lower values in the polar cap, compared with the auroral oval stations as reported by *Aarons* [1997], are a result of smaller irregularity amplitudes or smaller velocities. In the present study, with digisonde and spectral studies of scintillation, we could estimate the veloci-

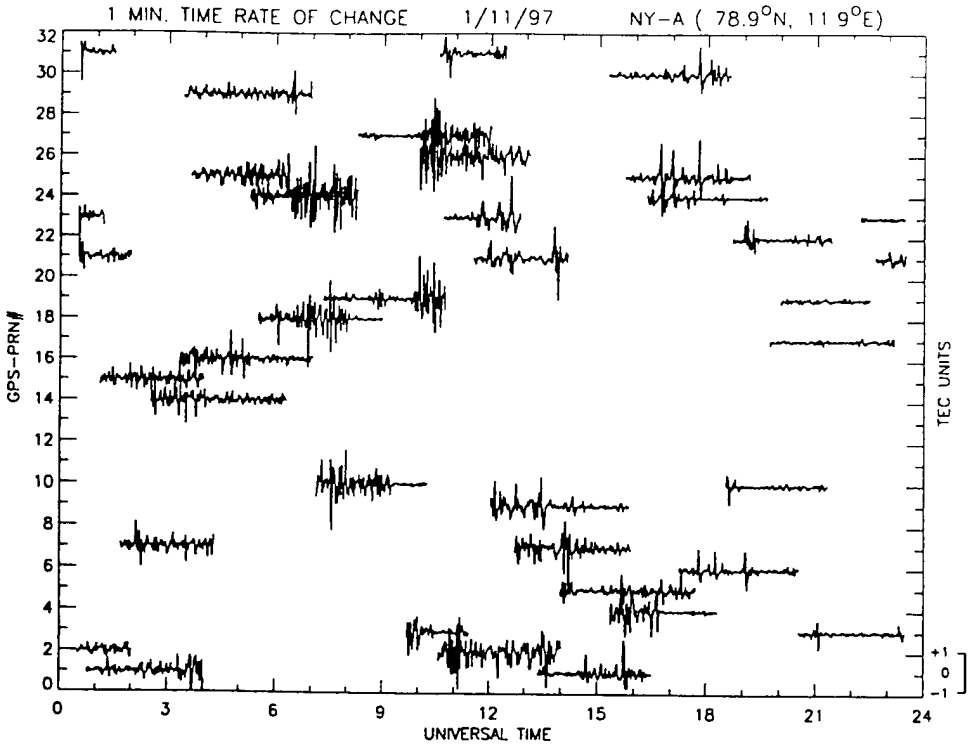

Figure 11. Shown are the rates of change of TEC as recorded by different satellites at Ny Alesund at different universal times during the magnetic storm period of January 11, 1997. The ordinate refers to prn of GPS satellites. The scale for the rate of change of TEC is indicated at the right bottom edge of the diagram.

ties and therefore determine the irregularity wavelengths with 30-s sampling of GPS carrier phase.

Amplitude scintillation measurements of GPS signals at 1.6 GHz were also conducted by using a receiver that recorded the signal amplitude at 50 Hz and processed on-line the S_4 scintillation index every 82 s. The amplitude scintillation data are plotted in Figure 12 in the same format as Figure 11. In this case, however, the separation between the successive horizontal lines corresponds to $S_4 = 0.25$. It may be seen that the receiver failed to detect any amplitude scintillation from a GPS satellite (prn 26). Some of the satellites, such as prn 23, show scintillation-like activity a little before 0900 UT. The events are not scintillation but are caused by multipath effects at low elevation angles encountered during the rise and set of the satellite. Unlike phase scintillations, where the irregularity wavelength sampled in an experiment depends on the velocity of the irregularities, amplitude scintillations are caused by irregularities in the range of the Fresnel dimension to a dimension smaller by about a decade. Thus, with irregularities at a range of 400 km, amplitude scintillations at the GPS frequency of 1.6 GHz are caused by irregularities in the wavelength range from 390 m, the Fresnel dimension, to about 30 m. These irregularity wavelengths (390–30 m) are 2–3 orders of magnitude smaller than those (36 km) detected by phase fluctuation measurements. Thus, in the presence of high ionospheric convection, the detection of large phase fluctuations may not signify the presence of smaller irregularities or be of sufficient strength to cause detectable levels of amplitude and phase scintillation.

4. Conclusions

Under solar minimum conditions of January 1997, weak ($S_4 < 0.4$) amplitude scintillations at 250 MHz were persistently observed during daytime at about 2° poleward of the nominal cusp region. Such scintillations, indicating the presence of subkilometer scale electron density irregularities, were observed not only

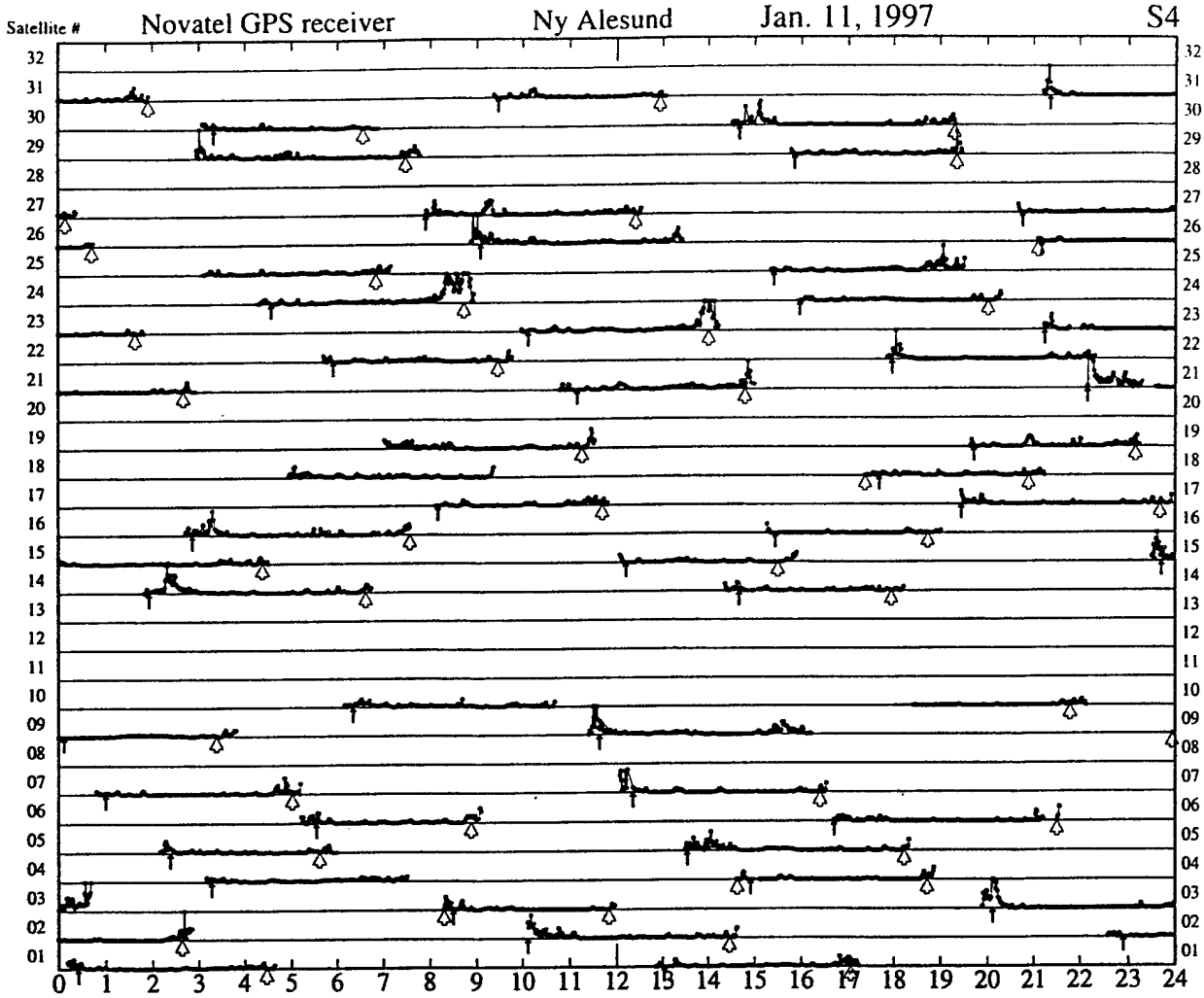

Figure 12. Shown is the amplitude scintillation at 1.6 GHz detected by different GPS satellites at different universal times during the magnetic storm period of January 11, 1997. The spacing between successive horizontal lines corresponds to an amplitude scintillation index of $S_4 = 0.25$. The figure shows that no amplitude scintillation was recorded. The scintillation-like variations are due to multipath effects which are encountered at low elevation angles.

near magnetic noon but also over much of the daytime, typically between 0900 MLT and 1500 MLT. The irregularities immediately poleward of the cusp may be convected from the proper cusp region or may be locally generated in the "cusp plume" region [*Newell et al.*, 1991]. The presence of irregularities in a longitudinally broad region slightly poleward of the cusp is probably related to the plasma mantle at low altitudes, which was first identified by *Newell et al.* [1991]. The discrete auroral features observed by these authors in this region and the associated field-aligned currents may be the source of the observed irregularities.

The dayside scintillation is characterized by frequency spectra which are generally broad but are occasionally interspersed by narrowband spectra. In our previous study in the cusp region at Sondrestrom, Greenland, we detected velocity shear and also observed broad frequency spectra of scintillations, implying the presence of turbulent plasma flows [*Basu et al.*, 1994]. This result was explained in terms of shear instabilities. *Baker et al.* [1995] have recently used

high-latitude HF radar data and established that the important radar characteristic of the cusp are the wide and complex Doppler power spectra. They recognized that plasma instability processes may impact the Doppler spectra but favored the alternative in which the wide spectra resulted from a structure within the $\mathbf{E} \times \mathbf{B}$ drift velocities. In this paper, we are reporting broad frequency spectra of scintillations poleward of the cusp region not only around magnetic noon but also away from noon. It is quite likely that in the presence of discrete auroral forms in the mantle [*Newell et al.*, 1991; *Murphree et al.*, 1990], shear instabilities may operate in this region and cause velocity turbulence in the nonlinear stage. This may also explain the observed broad frequency spectra of scintillation. *Ganguli et al.* [1994] have recently developed theories to show that a small amount of velocity shear in the transverse flow is sufficient to excite large-scale Kelvin-Helmholtz modes, which can nonlinearly steepen to excite microinstabilities that may energize ions.

We observed patches with small TEC enhancements only during the major magnetic storm. Modeling studies indicate that in view of the high geographic latitude of the cusp in the Ny Alesund sector, the corresponding polar cap patches and associated irregularities are weak and have low occurrence [*Basu et al.*, 1995]. We showed that at high latitudes in the presence of large convection speed, the IGS data sampled at 30-s intervals provide phase fluctuations at very large scales (40 km) and may not serve as an effective tracer of scintillation. With faster data sampling this IGS network may, however, be a very effective forecaster of scintillation.

Acknowledgments. We thank the staff of the Norsk Polarinstitut Research Station at Ny Alesund for their support during the January 1997 campaign and for continuous monitoring of the satellite receiving system. We gratefully acknowledge the help of JPL for supplying the GPS bias data. The work at Air Force Research Laboratory, Hanscom AFB, was partially supported by the Air Force Office of Scientific Research under task 2310G9.

References

Aarons, J., Global positioning system phase fluctuations at auroral latitudes, *J. Geophys. Res.*, *102*, 17,219, 1997.

Aarons, J., J. P. Mullen, H. Whitney, A. Johnson, and E. Weber, UHF scintillation activity over polar latitudes, *Geophys. Res. Lett.*, *8*, 277, 1981.

Aarons, J., M. Mendillo, R. Yantosca, and E. Kudeki, GPS phase fluctuations in the equatorial region during the MISETA campaign, *J. Geophys. Res.*, *101*, 26,851, 1996.

Baker, K. B., J. R. Dudeney, R. A. Greenwald, M. Pinnock, P. T. Newell, A. S. Rodger, N. Mattin, and C.-I. Meng, HF radar signatures of the cusp and low-latitude boundary layer, *J. Geophys. Res.*, *100*, 7671, 1995.

Basinska, E. M., W. J. Burke, N. C. Maynard, W. J. Hughes, J. D. Winningham, and W. B. Hanson, Small-scale electrodynamics of the cusp with northward interplanetary magnetic field, *J. Geophys. Res.*, *97*, 6369, 1992.

Basu, B., and B. Coppi, Plasma collective modes driven by velocity gradients, *J. Geophys. Res.*, *95*, 21,213, 1990.

Basu, S., Su. Basu, P. K. Chaturvedi, and C. M. Bryant Jr., Irregularity structures in the cusp/cleft and polar cap regions, *Radio Sci.*, *29*, 195, 1994.

Basu, S., Su. Basu, J. J. Sojka, R. W. Schunk, and E. MacKenzie, Macroscale modeling and mesoscale observations of plasma density structures in the polar cap, *Geophys. Res. Lett.*, *22*, 881, 1995.

Basu, Su., S. Basu, E. MacKenzie, and H. E. Whitney, Morphology of phase and intensity scintillations in the auroral oval and polar cap, *Radio Sci.*, *20*, 347, 1985.

Basu, Su., S. Basu, E. MacKenzie, P. F. Fougere, W. R. Coley, N. C. Maynard, J. D. Winningham, M. Sugiura, W. B. Hanson, and W. R. Hoegy, Simultaneous density and electric field fluctuation spectra associated with velocity shears in the auroral oval, *J. Geophys. Res.*, *93*, 115, 1988.

Buchau, J., B. W. Reinisch, E. J. Weber, and J. G. Moore, Structure and dynamics of the winter polar cap *F* region, *Radio Sci.*, *18*, 995, 1983.

Chaturvedi, P. K., and J. D. Huba, The interchange instability in high-latitude plasma blobs, *J. Geophys. Res.*, *92*, 3357, 1987.

Decker, D. T., C. E. Valladares, R. Sheehan, Su. Basu, D. N. Anderson, and R. A. Heelis, Modeling daytime *F* layer patches over Sondrestrom, *Radio Sci.*, *29*, 249, 1994.

Doherty, P., E. Raffi, J. Klobuchar, and M. B. El-Arini, Statistics of time rate of change of ionospheric range delay, in *Proceedings ION GPS-94*, p. 1589, Inst. of Navig., Alexandria, Va., 1994.

Ganguli, G., Y. C. Lee, P. J. Palmadesso, and S. L. Ossakow, Ion waves in a collisional magnetoplasma with a field-aligned current and a transverse velocity shear, in *Proceedings of the 1988 Cambridge Workshop in Theoretical Geoplasma Physics, Polar Cap Dynamics and High Latitude Ionospheric Turbulence*, pp. 231–242, Scientific, Cambridge, Mass., 1989.

Ganguli, G., M. J. Keskinen, H. Romero, R. Heelis, T. Moore, and C. Pollock, Coupling of microprocesses and macroprocesses due to velocity shear: An application to the low-altitude ionosphere, *J. Geophys. Res.*, *99*, 8873, 1994.

Kersley, L., C. D. Russell, and D. L. Rice, Phase scintilla-

tion and irregularities in the northern polar ionosphere, *Radio Sci.*, *30*, 619, 1995.

Keskinen, M. J., H. G. Mitchell, J. A. Fedder, P. Satyanarayana, S. T. Zalesak, and J. D. Huba, Nonlinear evolution of the Kelvin-Helmholtz instability in the high-latitude ionosphere, *J. Geophys. Res.*, *93*, 137, 1988.

Lotova, N. A., Temporal scintillation spectra with allowance for the solar-wind velocity distribution: Theory, *Geomagn. Aeron.*, *21*, 447, 1981.

Maynard, N. C., T. L. Aggson, E. M. Basinska, W. J. Burke, P. Craven, W. K. Peterson, M. Sugiura, and D. R. Weimer, Magnetospheric boundary dynamics: DE 1 and DE 2 observations near the magnetopause and cusp, *J. Geophys. Res.*, *96*, 3505, 1991.

Maynard, N. C., E. J. Weber, D. R. Weimer, J. Moen, T. Onsager, R. A. Heelis, and A. Egeland, How wide in magnetic local time is the cusp? An event study, *J. Geophys. Res.*, *102*, 4765, 1997.

Murphree, J. S., R. D. Elphinstone, D. Hearn, and L. L. Cogger, Large-scale high-latitude dayside auroral emissions, *J. Geophys. Res.*, *95*, 2345, 1990.

Newell, P. T., and C.-I. Meng, Mapping of the dayside ionosphere to the magnetosphere according to particle precipitation characteristics, *Geophys. Res. Lett.*, *19*, 609, 1992.

Newell, P. T., W. J. Burke, C.-I. Meng, E. R. Sanchez, and M. E. Greenspan, Identification and observations of the plasma mantle at low altitude, *J. Geophys. Res.*, *96*, 35, 1991.

Pi, X., A. J. Mannucci, U. J. Lindqwister, and C. M. Ho, Monitoring of global ionospheric irregularities using the worldwide GPS network, *Geophys. Res. Lett.*, *24*, 2283, 1997.

Sandholt, P. E., M. Lockwood, T. Oguti, S. W. H. Cowley, K. S. C. Freeman, B. Lybekk, A. Egeland, and D. M. Willis, Midday auroral breakup events and related energy and momentum transfer from the magnetosheath, *J. Geophys. Res.*, *95*, 1039, 1990.

Smith, M. F., and M. Lockwood, The pulsating cusp, *Geophys. Res. Lett.*, *17*, 1069, 1990.

Sojka, J. J., M. D. Bowline, and R. W. Schunk, Patches in the polar ionosphere: UT and seasonal dependence, *J. Geophys. Res.*, *99*, 14,959, 1994.

Tsunoda, R. T., High-latitude *F* region irregularities: A review and synthesis, *Rev. Geophys.*, *26*, 719, 1988.

Valladares, C. E., S. Basu, J. Buchau, and E. Friis-Christensen, Experimental evidence for the formation and entry of patches into the polar cap, *Radio Sci.*, *29*, 167, 1994.

Weber, E. J., J. Buchau, J. G. Moore, J. R. Sharber, R. C. Livingston, J. D. Winningham, and B. W. Reinisch, *F* layer ionization patches in the polar cap, *J. Geophys. Res.*, *89*, 1683, 1984.

Weber, E. J., J. A. Klobuchar, J. Buchau, H. C. Carlson Jr., R. C. Livingston, O. de la Beaujardiere, M. McCready, J. G. Moore, and G. J. Bishop, Polar cap *F* layer patches: Structure and dynamics, *J. Geophys. Res.*, *91*, 12,121, 1986.

S. Basu, J. Bongiolatti, T. W. Bullett, H. Kuenzler, and E. J. Weber, Air Force Research Laboratory, AFRL/VSBI, 29 Randolph Road, Hanscom Air Force Base, MA 01731. (e-mail: santimay@aol.com; bullett@plh.af.mil; webere@plh.af.mil)

P. Doherty, E. MacKenzie, and R. Sheehan, Institute for Scientific Research, Boston College, Newton, MA 02159.

M. J. Keskinen, Plasma Physics Division, Naval Research Laboratory, 4555 Overlook Avenue, SW, Washington, D. C. 20375. (keskinen@ppd.nrl.navy.mil)

P. Ning, KEO Consultants, 24 Brookline Avenue, Brookline, MA 02146.

(Received January 19, 1998; revised May 5, 1998; accepted May 8, 1998.)